

NUMERICAL STUDY OF A LASER-DRIVEN GRATING-BASED DIELECTRIC ACCELERATOR*

Zhaofu Chen[†], Hayato Okamoto, The University of Tokyo, Tokyo, Japan
Kazuyoshi Koyama, Mitsuru Uesaka, The University of Tokyo, Tokai, Japan
Mitsuhiro Yoshida, High Energy Accelerator Research Organization, Tsukuba, Japan

Abstract

Dielectric laser acceleration of electrons has been demonstrated recently with the potential to miniaturize accelerator due to its high gradient. Here we present a numerical investigation of a grating-based dielectric laser accelerator designed for nonrelativistic electrons which can be used in radiobiology research. We optimize the structure and discuss the electric field in the vicinity of the grating. We show the simulation results for a single electron and a DC electron beam interacting with such field.

INTRODUCTION

The dielectric laser accelerators (DLAs) have attracted increasing interest in the recent years due to their potential to reduce the size and cost of the conventional radio-frequency (RF) accelerators [1, 2]. Due to the damage threshold of the metal cavities, the radio-frequency accelerators typically operate at acceleration gradient of 10 to 50 MV/m but gradient up to 100 MV/m has been demonstrated to be reachable. By comparison, the damage thresholds of dielectric materials in optical region, such as silica, sapphire, and silicon, are 1 to 2 orders of magnitude higher than the typical gradients of the metallic structures. By leveraging the high damage threshold of dielectric materials, DLAs can reach gradient of GV/m level. Recently, acceleration gradient of 690 MeV/m have been achieved in the dual grating structure for relativistic electrons[3, 4], and acceleration gradients of 25 MeV/m, 220 MeV/m and 370 MeV/m have been demonstrated with silica single grating, silicon single grating, and silicon dual pillar grating for nonrelativistic electrons[5-7].

Described here is a grating-based DLA for radiobiology research. The damage effect of low radiation doses on the living cell is important for cancer radiation treatment, nuclear accident and radiobiological terrorism. Irradiation of the living cell with charged particle beam, such as an electron beam with energy 1 MeV and bunch charge 0.01 fC, is an useful method to study the radiobiological processes and evaluate the cancer risks of low dose radiation[8]. DLA is suitable for this application since it can deliver nanometre-sized beams with attosecond pulse width. Here, we introduce simulation results of a grating structure for acceleration of nonrelativistic electrons[9].

STRUCTURE GEOMETRY

The single grating and its work principle are shown in Figure 1. The period of grating is λ_p , the pillar height H_p , the groove width W_g , and the distance between the electron beam and the grating surface d . The incoming TM mode laser is fed from below at normal incidence to the grating

surface, with the electric field polarized along the electron propagation direction. The evanescent fields are generated in the vicinity of the grating, in which one of the spatial harmonic is designed to have a phase velocity synchronous with the electrons travelling above the grating so that the electrons can be accelerated continuously.

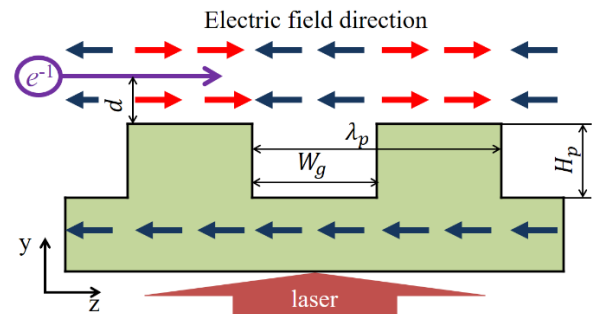


Figure 1: Principle of the single grating accelerator.

For electrons with velocity $\beta = v/c$ travel above the grating driven by a laser with wavelength λ_0 , the period of grating should be set as $\lambda_p = n\beta\lambda_0$, so that the n th order spatial harmonic can be utilized to accelerate the electrons.

In the simulation, a laser of wavelength $\lambda_0 = 1030$ nm is used to drive the structure. Fused silica, with a refractive index of 1.45, is chosen to be the grating material with a damage threshold 3.5 J/cm². We assume the initial energy of nonrelativistic electrons to be 50 keV, corresponding to a velocity relative to the speed of light as $\beta = 0.41$. To utilize the first spatial harmonic to accelerate electrons, the period of grating should be set as $\lambda_p = 425$ nm. The other dimensions will be determined in the simulation.

FIELD DISTRIBUTION

To determine the optimum geometry, we use the CST Microwave Studio. Only one period of grating is modelled in the field simulation, with periodic boundary conditions in Z direction, and open boundary conditions in Y direction. The thickness of the grating in X direction is set to be one wavelength of the plane wave. The mesh coarseness is $\lambda_0/40$. The simulation method has been verified by comparing the results with the data from the literature.

The crucial character of DLA is the high acceleration gradient limited by the damage threshold of the dielectric material. The acceleration gradient G_{acc} and deflection gradient G_{defl} are defined as the average electromagnetic field experienced by electrons over one period of grating in the longitudinal direction and lateral direction respectively, which are given by:

$$G_{acc} = \frac{1}{\lambda_p} \int_0^{\lambda_p} E_z[z(t), t] dz \quad (1)$$

$$G_{defl} = \frac{1}{\lambda_p} \int_0^{\lambda_p} (E_y[z(t), t] + vB_x[z(t), t]) dz \quad (2)$$

here $E_z[z(t), t]$, $E_y[z(t), t]$ and $B_x[z(t), t]$ are z component of electric field, y component of electric field and x component of magnetic field experienced by the electrons at position $z(t)$ and time t respectively. The maximum electric field in the grating material is enhanced by an enhancement factor f to $E_p = fE_0$, where E_0 is the peak electric field of the incident laser. If the DLA operates in region when gradient is limited by the electric field of incident laser, the structure should be designed so that the normalized acceleration gradient $\epsilon_{acc} = G_{acc}/E_0$ is maximized. If DLA operates close to the maximum acceleration gradient which is limited by the damage threshold of the grating material, the figure of merit is the ratio between the gradient and the maximum electric field in the grating material, known as acceleration factor $\eta_{acc} = G_{acc}/E_p$.

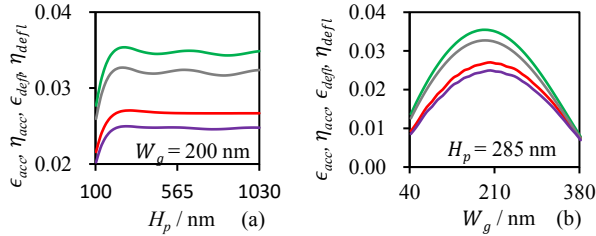


Figure 2: The amplitude of normalized acceleration gradient ϵ_{acc} (green), acceleration factor η_{acc} (red), normalized deflection gradient ϵ_{defl} (grey) and deflection factor η_{defl} (purple) as a function of the pillar height (a), and the groove width (b).

Figure 2 shows the normalized acceleration gradient ϵ_{acc} and the acceleration factor η_{acc} at a beam-grating distance of 100 nm as a function of pillar height H_p and groove width W_g respectively. The maximum normalized acceleration gradient and acceleration factor appears at different location. The maximum acceleration factor 0.028 occurs at pillar height $H_p = 285$ nm and trench width $W_g = 200$ nm, while the maximum normalized acceleration gradient occurs at pillar height $H_p = 260$ nm and groove width $W_g = 190$ nm. In our design, we seek after the maximum acceleration gradient without damage, so we choose the optimum structure with maximum acceleration factor. The enhancement factor f and normalized gradient ϵ_{acc} in the optimum structure are 1.31 and 0.036 respectively.

Figure 3 shows the longitudinal electric field normalized to the electric field of the incident laser in the YZ plane with the optimum structure when the plane wave is launched from below. The electric field above the grating is the combination of the harmonics, and only the first order spatial harmonic satisfies the synchronicity condition and can accelerate electrons continuously. The maximum longitudinal electric field is located around the corner of the pillar.

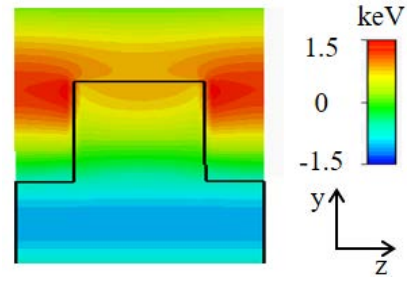


Figure 3: Distribution of the longitudinal electric field normalized to the incident laser electric field in the YZ plane.

The dependencies of acceleration gradient and deflection gradient on the start phase in the optical cycle when the electron arrives at the grating are shown by Figure 4(a), in which the initial electron-grating distance $d = 100$ nm. To efficiently accelerate the electrons, the electrons should arrive at the grating at the optimum acceleration phase $\theta = 0$ rad. The lateral deflection force is the Lorentz force in the Y direction exerted by E_y and B_x . It is shown that the deflection and acceleration are 90 degrees out of phase. For an electron arriving at the optimum accelerating phase, it will gain maximum energy but experience minimal deflection[10].

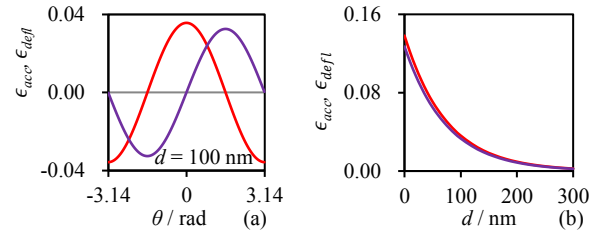


Figure 4: The amplitude of normalized acceleration gradient (red) and deflection gradient (purple) as a function of start phase θ (a) and electron-grating distance d .

Figure 4(b) shows the amplitude of acceleration factor η_{acc} and deflection factor η_{defl} as a function of electron-grating distance d . The working mode is an evanescent mode, so the acceleration gradient and deflection gradient fall off exponentially with the electron-grating distance. If the distance is too far, the acceleration gradient becomes zero and the electron will not be accelerated. For an e-beam with non-zero transverse dimension, acceleration force and deflection force on electrons vary with the electron-grating distance, leading to the distortion of the electron beam, which can be solved by using dual grating structure illuminated by two opposite lasers.

ACCELERATION OF ELECTRONS

To study the electrons' behaviour in the accelerator, we perform PIC simulation with CST Particle Studio. For a 50 keV electron injected into the structure with 10 periods of grating at a distance of 100 nm, the energy and position of the electron are shown in Figure 5, in which we also show the energy gain predicted by field simulation with $G_{acc} = 0.035E_0$. The peak electric field of the incident plane wave is $E_0 = 10$ GV/m. The electron gains energy

along z axis while being slightly deflected. In the first two periods, PIC simulation results is in agreement with the field simulation results, but in the downstream several periods, there is a growing distinction. We infer that the distinction is the result of the reduction of acceleration gradient due to dephasing process, which can be solved by changing the grating's period or laser's wavelength in accordance with electron energy[11].

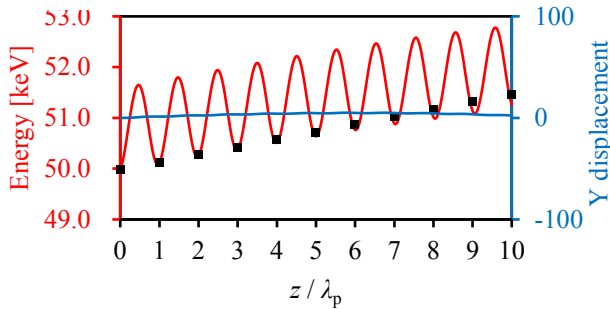


Figure 5: The comparison of PIC simulation results (red: energy, blue: displacement in Y direction) for an electron injected at the optimum accelerating phase with field simulation results (black dots: energy of electron predicted by $G_{acc} = 0.035E_0$).

For a DC 50 keV electron beam with infinitely small transverse size injected into the structure which includes 10 periods of grating at a distance of 100 nm, Figure 6 shows the PIC simulation results of energy and position of electrons. The electron beam is energy modulated, in which the energy gain depends on the start phase of the electron. In the later several periods, electrons with higher velocity will catch up with electrons with lower velocity, leading to density modulation of electrons, and electron bunches are being formed. Despite the dephasing and deflection, those electrons with relatively higher energy gain are deflected less significantly, indicating that the acceleration and deflection are about 90 degrees out of phase, which is in agreement with the field simulation result.

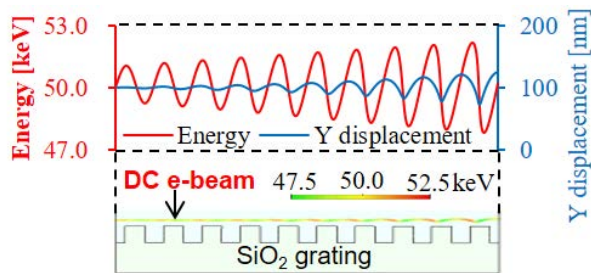


Figure 6: The PIC simulation results for a DC electron beam (colourful curve: snapshot of energy and position of electrons, red: energy, blue: Y displacement).

CONCLUSION

The numerical investigation of a grating-based DLA for 50 keV nonrelativistic electrons is presented. The structure is expected to produce a maximum gradient of 0.036 times the peak electric field of incident laser. In a multi-period grating, the dephasing and deflection process lead to the

reduction of acceleration gradient and result in a lower energy gain. Low energy DLAs could be used for the radiobiology research as charged particle beam sources to evaluate the effect of low dose radiation on the damage process of a living cell. High energy DLAs could be used for the light sources and colliders.

ACKNOWLEDGEMENT

We thank S. Otsuki, T. Shibuya, R. Zhang, T. Natsui and A. Inoue for helpful discussions. This work is supported by KAKENHI, Grant-in-Aid for Scientific Research (B) 15H03595.

REFERENCES

- [1] R. J. England *et al.*, "Dielectric laser accelerators", *Rev. Mod. Phys.*, vol. 86, no. 4, pp. 1337-1389, 2014.
- [2] R. J. England, "Review of Laser-Driven Photonic Structure-Based Particle Acceleration," *IEEE J. Sel. Top. QUANTUM Electron.*, vol. 22, no. 2, 2016.
- [3] K. P. Wootton *et al.*, "Demonstration of acceleration of relativistic electrons at a dielectric microstructure using femtosecond laser pulses", *Opt. Lett.*, vol. 41, no. 12, pp. 2696-2699, Jun. 2016.
- [4] E. A. Peralta *et al.*, "Demonstration of electron acceleration in a laser-driven dielectric microstructure", *Nature*, 2013.
- [5] K. J. Leedle *et al.*, "Laser acceleration and deflection of 96.3 keV electrons with a silicon dielectric structure", *Optica*, vol. 2, no. 2, pp. 158-161, 2015.
- [6] K. J. Leedle *et al.*, "Dielectric laser acceleration of sub-100 keV electrons with silicon dual-pillar grating structures", *Opt. Lett.*, vol. 40, no. 18, pp. 4344-4347, 2015.
- [7] J. Breuer and P. Hommelhoff, "Laser-Based Acceleration of Nonrelativistic Electrons at a Dielectric Structure", *Phys. Rev. Lett.*, vol. 111, no. 13, p. 134803, 2013.
- [8] K. Koyama *et al.*, "Parameter study of a laser-driven dielectric accelerator for radiobiology research," *J. Phys. B At. Mol. Opt. Phys.*, vol. 47, no. 23, p. 234005, 2014.
- [9] J. Breuer, J. McNeur, and P. Hommelhoff, "Dielectric laser acceleration of electrons in the vicinity of single and double grating structures—theory and simulations", *J. Phys. B At. Mol. Opt. Phys.*, vol. 47, no. 23, p. 234004, 2014.
- [10] T. Plettner, R. L. Byer, and B. Montazeri, "Electromagnetic forces in the vacuum region of laser-driven layered grating structures," *J. Mod. Opt.*, vol. 58, no. 17, pp. 1518-1528, 2011.
- [11] Martin Kozák *et al.*, "Transverse and longitudinal characterization of electron beams using interaction with optical near-fields," *Opt. Lett.*, vol. 41, no. 15, pp. 3435-3438, 2016.